J Mater Sci (2006) 41:7040–7044
DOI 10.1007/s10853-006-0949-z

Oxidation behavior of silicon nitride sintered with Lu_2O_3 additive

Madeleine K. Jordache · Henry Du

Received: 31 March 2005 / Accepted: 22 December 2005 / Published online: 20 October 2006

Abstract Kyocera SN282 silicon nitride ceramics sintered with 5.35 wt% Lu_2O_3 were oxidized in dry oxygen at 930–1,200 °C. Oxidation of SN282 follows a parabolic rate law. SN282 exhibits significantly lower parabolic rate constants and better oxide morphological stability than silicon nitride containing other sintering additives under similar conditions. The activation energy for oxidation of SN282 is 107 ± 5 kJ/mol K, suggesting inward diffusion of molecular oxygen in the oxide layer as the rate-limiting mechanism.

Introduction

A large variety of sintering additives have been explored for densification and optimization of mechanical properties of silicon nitride for advanced engineering applications such as advanced turbines for aero-propulsion and electric power generation. Addition of sintering aids is almost always at the expense of the high-temperature oxidation resistance of silicon nitride, as documented in numerous studies [1–4]. It is generally observed that during oxidation, concomitantly with the growth of the thermal oxide on the ceramic surface, additive and impurity cations diffuse via ceramic grain boundaries to the oxide layer. This diffusion process leads to formation of oxides whose chemistry and transport properties deviate significantly from those of silica. The consequence is an increased rate of oxidation and reduced oxide morphological stability. The oxidation rate of silicon nitride is often dictated by the type and the amount of sintering additives, with outward diffusion of the additive cations as the main rate-controlling mechanism [5–9].

Rare-earth oxides have been increasingly used to facilitate the densification of silicon nitride with promising outcome both in terms of high-temperature mechanical properties and environmental stability [10–15]. The crystalline nature of the grain boundary phases in which these additives reside is a major contributor to the enhanced performance of silicon nitride ceramics. For example, silicon nitride ceramics containing Er_2O_3, Y_2O_3, Yb_2O_3 and La_2O_3 as additives were reported to show favorable oxidation resistance, with Er_2O_3 additive resulting in the best oxidation resistance due to the high ionic field strength of Er^{+3} and the high eutectic temperature of the Er_2O_3–SiO_2 system [4]. Lu_2O_3 additive has also been shown to yield silicon nitride ceramics of robust oxidation resistance [11–13]. Oxidation of this type of ceramic was reported to follow a parabolic rate law, indicating a diffusion-controlled oxidation process, though no specific rate-limiting mechanism has been suggested for the oxidation.

This paper reports an oxidation study of a turbine-grade Kyocera SN282 Si_3N_4 sintered with Lu_2O_3. The oxidation kinetics and the phase and morphological characteristics of the oxides are examined with temperature as a parameter. The mechanism of oxidation is discussed based on experimental findings.

M. K. Jordache (✉) · H. Du
Department of Chemical, Biomedical and Materials Engineering, Stevens Institute of Technology, Hoboken, NJ 07030, USA
e-mail: mjordach@stevens.edu

Experimental procedure

SN282 was obtained from Kyocera Industrial Ceramics Corp. It was fabricated by cold isostatic pressing of Si_3N_4 powders with ~5.35 wt% Lu_2O_3 for improved green density followed by reactive sintering. Impurities present in SN282 are: Yb_2O_3 (0.058 wt.%), Na_2O (0.053 wt%), Al_2O_3 (0.045 wt%), CaO (0.016 wt%), and MgO (0.002 wt%), according to the vendor. The resultant ceramic is β-Si_3N_4 with crystalline grain boundary phases consisting of $Lu_2Si_2O_7$ and traces of Lu_2SiO_5. SN282 platelets were tribochemically polished in a 3 wt% chromium trioxide aqueous solution using an SX tribo-machine (Axis Industrial Automation, Somerville, NJ) to a surface finish with a measured root mean square roughness of about 5 nm. The polished samples were ultrasonically cleaned in de-ionized water, acetone, and methanol to remove surface contaminants before oxidation.

Oxidation experiments were conducted in 1 atm dry oxygen flowing at 500 SCCM at 930–1,200 °C for durations up to 20 h using a horizontal alumina tube-furnace (CM Furnaces, Bloomfield, NJ). Oxide thickness was measured using a Leo 982 field-emission-gun scanning electron microscope (SEM) (Leo Microscopy, Thornwood, NY) in a cross-sectional geometry and a Talysurf 10 profilometer (Rank Taylor Hobson, Des Plaines, IL) in conjunction with etch patterning in buffered NH_4F:HF (10:1) solution. The morphological, chemical, and phase characteristics of the oxide were determined by SEM in conjunction with energy dispersive x-ray analysis (EDX) and by x-ray diffraction (XRD) using a Siemens D 5000 x-ray diffractometer.

Results

Shown in Fig. 1 is the time dependence of oxide thickness with temperature as a parameter for oxidation of SN282 at 930–1,200 °C. The error bars arise from the scattering of thickness values from typically five measurements. The thickness-time correlation fits well with a parabolic relation for all temperatures, according to least square analysis. Summarized in Table 1 are parabolic rate constants for oxidation of SN282. Illustrated in Fig. 2 is the Arrhenius plot between the parabolic rate constants and the oxidation temperature. The slope value of the straight line yields an apparent activation energy of 107 ± 5 kJ/mol K for oxidation of SN282 at 930–1,200 °C.

Presented in Fig. 3 are XRD patterns from SN282 samples oxidized at 930–1,200 °C for 20 h. The XRD pattern of as-received SN282 is also included for comparison. Diffraction peaks corresponding to β-Si_3N_4, $Lu_2Si_2O_7$, and to a lesser extent Lu_2SiO_5 are seen in the as-received SN282 sample. $Lu_2Si_2O_7$ and Lu_2SiO_5, residing mainly at triple-grain junctions, are reaction products between Si_3N_4 and Lu_2O_3 additive during reactive sintering. Oxidation under the conditions investigated did not result in identifiable changes in terms of the constituent crystalline phases, except for the notable presence of cristobalite in samples oxidized at 1,200 °C.

Shown in Fig. 4 are SEM micrographs of SN282 samples before and after oxidation at 1,000, 1,100, and 1,200 °C for 20 h. The surface morphology of the unoxidized sample in Fig. 4a reveals discrete regions of light contrast in an otherwise featureless surface due to high surface finish. Etching of the polished surface and analysis by XRD and EDX indicated that the discrete phases are mainly of $Lu_2Si_2O_7$ and traces of Lu_2SiO_5 situated in the triple grain junctions of silicon nitride grains. The image contrast, size and distribution of the discrete phases in the unoxidized sample are generally preserved in samples after oxidation as seen in Figs. 4b–d. Shown in Fig. 5 are EDX spectra taken from the regions of light and dark contrast of the

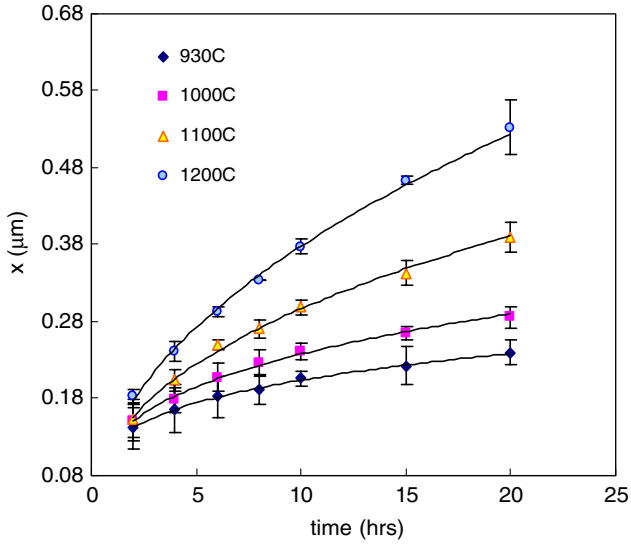

Fig. 1 Oxide thickness as a function of oxidation time for SN282 at 930–1,200 °C in dry O_2

Table 1. Parabolic rate constants for oxidation of SN282 in dry O_2

T (°C)	k_p (μm^2/h)
930	$0.002 \pm 1.5 \times 10^{-4}$
1,000	$0.0032 \pm 2.8 \times 10^{-4}$
1,100	$0.0069 \pm 2.9 \times 10^{-4}$
1,200	$0.014 \pm 1.5 \times 10^{-4}$

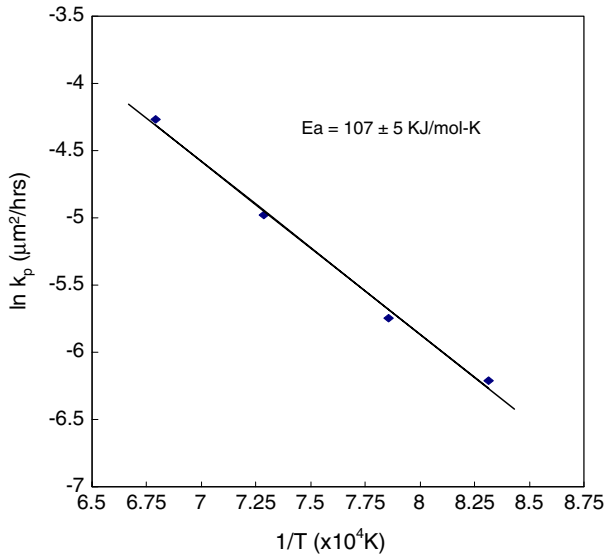

Fig. 2 Arrhenius plot of parabolic rate constants for oxidation of SN282 at 930–1,200 °C in dry O_2

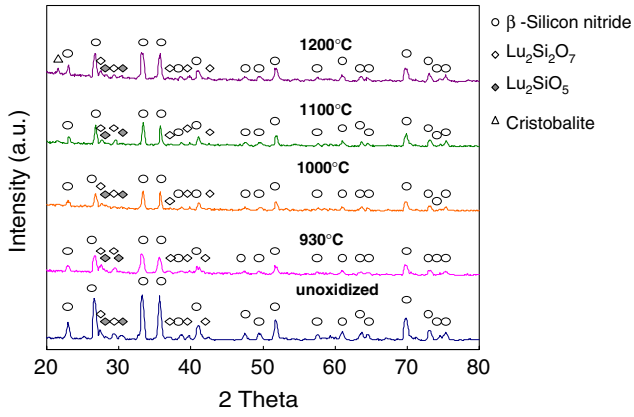

Fig. 3 XRD spectra from SN282 before and after oxidation at 930–1,200 °C in dry O_2 for 20 h

sample exhibited in Fig. 4d. Clearly, the discrete phases are rich in Lu, Si, and O and are mainly crystalline $Lu_2Si_2O_7$, based on both EDX and XRD of SN282 oxidized between 930–1,200 °C. The region of the dark contrast is basically silica. It is interesting to note that the size and distribution of the dominant $Lu_2Si_2O_7$ phases do not exhibit an apparent dependence on oxidation temperature. A major morphological difference exists, however, between unoxidized and oxidized samples in that, as oxidation conditions intensified (e.g., via increased oxidation temperature), the discrete $Lu_2Si_2O_7$ phases raised above otherwise a smooth oxide layer. This feature is vividly illustrated in Fig. 6, an SEM cross section of SN282 oxidized at 1,200 °C for 15 h. One $Lu_2Si_2O_7$ grain, as marked by the arrow, can be seen to be lodged in a dense oxide layer right at the cross section whereas many other grains are visible in the background.

Discussion

Oxidation of SN 282 followed a parabolic type rate law, indicating diffusion-controlled oxidation mechanism. Compared to silicon nitride ceramics sintered with other additives (such as Y_2O_3 and MgO) [3, 6, 9], SN282 exhibits a far lower oxidation rate with an apparent activation energy close to that for molecular oxygen diffusion in silica [16]. The thermally grown oxide is highly protective to the Si_3N_4 substrate beneath; it is a dense, amorphous silica layer embedded with discrete and stable $Lu_2Si_2O_7$ grains.

Based on the apparent activation energy and the nature of the oxide layer grown during oxidation, it is plausible that oxidation of SN282 is rate-limited by

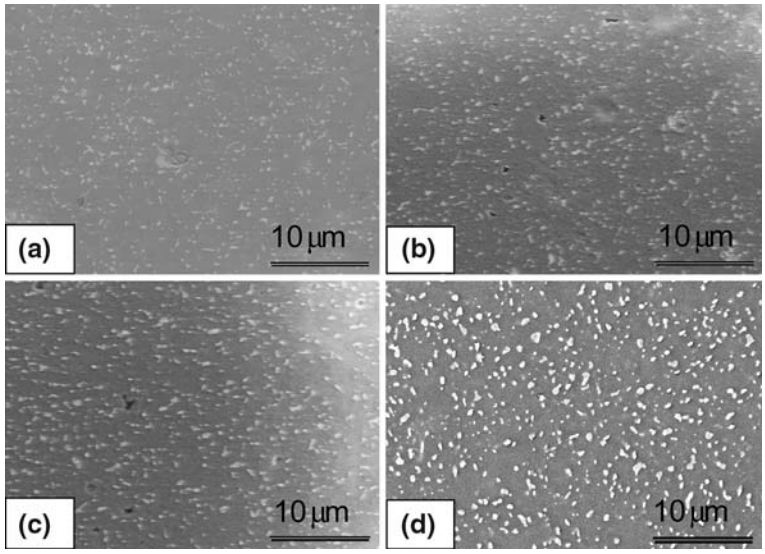

Fig. 4 SEM micrographs of SN282 (**a**) before oxidation and after oxidation at (**b**) 1,000 °C, (**c**) 1,100 °C, and (**d**) 1,200 °C in dry O_2 for 20 h

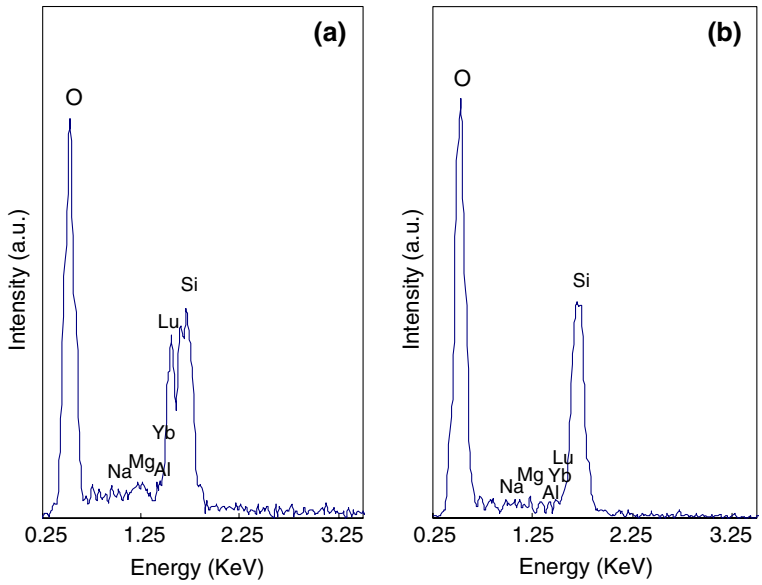

Fig. 5 EDX spectrum from (**a**) the discrete phase region of light contrast and (**b**) the region of dark contrast of oxidized SN282 exhibited in Fig. 4(**d**)

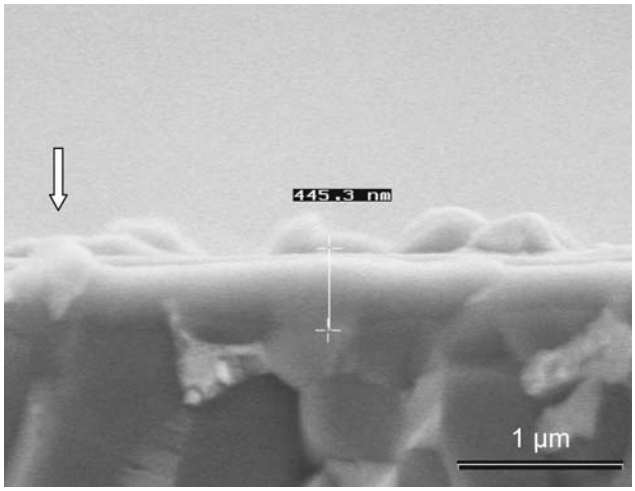

Fig. 6 SEM cross-section of SN282 oxidized at 1,200 °C in dry O_2 for 15 h

inward diffusion of oxygen through the oxide layer to the ceramic substrate in the temperature range of 930–1,200 °C we investigated. The oxidation mechanism suggested here for SN282 clearly deviates from the general mechanistic assessment of oxidation of additive-containing Si_3N_4 ceramics where outward diffusion of additive cations through the ceramic grain boundaries to the oxide layer is often the rate-limiting process.

In order for outward diffusion of additive cations via ceramic grain boundaries, as opposed to inward diffusion of oxygen through the oxide layer, to be operative as the rate-limiting step, the following two conditions need to be satisfied. First, additive cations should be sufficiently mobile so as to result in appreciable enrichment in the oxide layer. Second, the nature of the oxide layer should be modified by the additive cations so that oxygen diffusion is significantly accelerated. These conditions are not in place in the case of SN282. For instance, according to Fig. 4, the size and density of discrete $Lu_2Si_2O_7$ particles in the surface region of the oxide layers clearly coincide with those of the secondary phases in the surface region of the as-received ceramic substrate. This observation as well as the temperature independence of the particle sizes points strongly to the fact that $Lu_2Si_2O_7$ is a very stable phase in the $Lu_2Si_2O_7$–SiO_2 system under current conditions. There is no appreciable outward grain boundary diffusion of Lu^{3+}. The phase and chemical characteristics of SiO_2 as well as oxygen diffusion were not altered in any substantial way by the inclusion of stable $Lu_2Si_2O_7$ as reflected by the absence of other adverse morphological features in the oxide layers, apart from the discrete $Lu_2Si_2O_7$ particles.

The discrete $Lu_2Si_2O_7$ phases became lodged in the oxide layer as the conversion of silicon nitride to silicon dioxide continued. The extruding nature of the $Lu_2Si_2O_7$ grains can be attributed to a combination of (1) grain boundary oxidation of Si_3N_4 and associated volume expansion of oxide in the triple grain junction regions and (2) minimization of surface stress and surface free energy in a multiphase system.

Overall, the excellent oxidation resistance of SN282 can be attributed to the presence of a crystalline and refractory grain boundary phase, where outward diffusion of additive cations is minimal. The protective nature of the oxide layer formed is not adversely affected by the presence of the $Lu_2Si_2O_7$ phase. It needs to be noted that a higher activation energy value of 204 KJ/mol has been reported [13] for oxidation of SN282 in dry oxygen at 1,200–1,400 °C. A similar value

could also be obtained via extrapolation of the results from an oxidation study of Si_3N_4 sintered with 3.33 wt% Lu_2O_3 additive at 1,400–1,500 °C [12]. It is highly probable that above 1,200 °C, a different oxidation mechanism may become operative for SN282, such as a mixture of network exchange diffusion and molecular oxygen diffusion in the oxide layer or outward diffusion of additive cations in the ceramic substrate. Temperature-dependent oxidation mechanism has been well-documented for silica-forming materials such as SiC [17].

Conclusions

(1) SN282 follows a parabolic oxidation rate law in the temperature range of 930–1200 °C. It is considerably more stable than silicon nitride sintered with other additives.
(2) The oxide layer consists of mainly amorphous silica embedded with discrete $Lu_2Si_2O_7$ grains. The distribution of the $Lu_2Si_2O_7$ grains corresponds to that at the triple grain junctions of SN282.
(3) Oxidation of SN282 in the temperature range investigated is probably rate-limited by molecular oxygen diffusion in the silica phase of the oxide layer, in contrast to the outward diffusion of cations mechanism commonly observed for other additive-containing Si_3N_4 ceramics.

References

1. Quakenbush CL, Smith JT (1980) Am Ceram Soc Bull 59: 533
2. Gogotsi YG, Grathwohl G, Thummler F, Yaroshenko VP, Herrman M, Taut C (1993) J Europ Ceram Soc 11: 375
3. Mukundhan P, Jianqing Wu, Henry HDu (1999) J Am Ceram Soc 82: 2260
4. Choi HJ, Lee JG, Kim YW (1999) J Europ Ceram Soc 19: 2757
5. Clarke DR, Lange FF (1980) J Am Ceram Soc 63: 586
6. Cubicciotti D, Lau KH (1977) J Am Ceram Soc 61: 512
7. Mieskowski DM, Sanders WA (1985) J Am Ceram Soc 68: C–160
8. Babini GN, Bellosi A, Vincenzini P (1981) Sci Ceram 11: 291
9. Cubicciotti D, Lau KH (1979) J Eletrochem Soc 126: 1723
10. Cinibulk MK, Thomas G, Johnson SM (1992) J Am Ceram Soc 75: 2050
11. Choi HJ, Lee JG, Kim YW (1997) J Mater Sci 32: 1937
12. Guo S, Hirosaki N, Yamamoto Y, Nishimura T, Mitomo M (2002) J Am Ceram Soc 85: 1607
13. Fox DS, Opila EJ, Nguyen QN, Humphrey DL, Lewton SM (2003) J Am Ceram Soc 86: 1256
14. Guo S, Hirosaki N, Nishimura T, Yamamoto Y, Mitomo M (2002) Phil Mag A 82: 3027
15. Maeda M, Nakamura K, Yamada M (1990) J Mater Sci 25: 3790
16. Deal BE, Grove AS (1965) J Appl Phys 16: 3770
17. Jacobson NS (1993) J Am Ceram Soc 76: 3